

# Thermally driven self-healing using copper nanofiber heater

Min Wook Lee, Hong Seok Jo, Sam S. Yoon, and Alexander L. Yarin

Citation: *Appl. Phys. Lett.* **111**, 011902 (2017); doi: 10.1063/1.4990962

View online: <http://dx.doi.org/10.1063/1.4990962>

View Table of Contents: <http://aip.scitation.org/toc/apl/111/1>

Published by the [American Institute of Physics](#)

---

---



**THE WORLD'S RESOURCE FOR  
VARIABLE TEMPERATURE  
SOLID STATE CHARACTERIZATION**



OPTICAL STUDIES SYSTEMS



SEEBECK STUDIES SYSTEMS



MICROPROBE STATIONS



HALL EFFECT STUDY SYSTEMS AND MAGNETS



[WWW.MMR-TECH.COM](http://WWW.MMR-TECH.COM)

## Thermally driven self-healing using copper nanofiber heater

Min Wook Lee,<sup>1,2,a)</sup> Hong Seok Jo,<sup>3,a)</sup> Sam S. Yoon,<sup>3,b)</sup> and Alexander L. Yarin<sup>1,b)</sup>

<sup>1</sup>Department of Mechanical and Industrial Engineering, University of Illinois at Chicago, 842 W. Taylor St., Chicago, Illinois 60607-7022, USA

<sup>2</sup>Multifunctional Structural Composite Research Center, Institute of Advanced Composites Materials, Korea Institute of Science and Technology, Chudong-ro 92, Bondong-eup, Wanju-gun, Jeollabuk-do 55324, South Korea

<sup>3</sup>School of Mechanical Engineering, Korea University, Seoul 136-713, South Korea

(Received 21 May 2017; accepted 17 June 2017; published online 5 July 2017)

Nano-textured transparent heaters made of copper nanofibers (CuNFs) are used to facilitate accelerated self-healing of bromobutyl rubber (BIIR). The heater and BIIR layer are separately deposited on each side of a transparent flexible polyethylene terephthalate (PET) substrate. A pre-notched crack on the BIIR layer was bridged due to heating facilitated by CuNFs. In the corrosion test, a cracked BIIR layer covered a steel substrate. An accelerated self-healing of the crack due to the transparent copper nanofiber heater facilitated an anti-corrosion protective effect of the BIIR layer. *Published by AIP Publishing.* [<http://dx.doi.org/10.1063/1.4990962>]

Transparent conducting electrodes are widely used in LED (light emitting diodes),<sup>1</sup> touch screens,<sup>2</sup> displays,<sup>3</sup> etc. The electrode films made of metal, carbon nanotubes (CNTs), and graphene are manufactured by CVD (chemical vapor deposition),<sup>2</sup> vacuum filtration,<sup>4</sup> calcination,<sup>5</sup> electroplating,<sup>6,7</sup> supersonic blowing,<sup>8,9</sup> etc. Similar transparent electrode coatings can be developed for heaters, which convert the electrical energy into thermal energy via Joule heating. Hong *et al.*<sup>10</sup> demonstrated stretchable (up to 60%), transparent heaters made of silver nanowires (AgNWs). Lee *et al.*<sup>11</sup> sprayed AgNW solution in supersonic gas flow and formed a self-fused AgNW network which could be used as a transparent heater with the temperature rise up to 160 °C at the applied voltage of 8 V, with the 15 Ω/sq sheet resistance and 95% transparency. The latter transparent heater was thermally and mechanically stable after the repeated bending test for 600 000 cycles.

External stimuli such as heat,<sup>12–15</sup> UV/visible light,<sup>16–19</sup> and pH<sup>20,21</sup> can assist self-healing of engineered materials when energy supply is available. This is a disadvantage compared to the autonomous self-healing strategy. However, thermally self-healing materials, with an unlimited recyclability and full recovery, are still attractive and thus in focus.<sup>22</sup>

Bromobutyl rubber (BIIR) is the material mostly used for automobile tires. Das *et al.* showed that two fully cut pieces of ionic-modified BIIR can be reassembled to restore the original mechanical properties (the elastic modulus, tensile strength, and ductility), which is understood as full self-healing.<sup>23</sup> The segments of the rubber network are rearranged due to the dynamic ionic association, thus inducing physical cross-linking of isobutylene and isoprene with the aid of allylic bromide groups (see Fig. 1). This reversible self-healing feature of bromobutyl rubber can be enhanced at elevated temperature. The use of a flexible, transparent thin-film heater facilitating thermally driven self-healing of a soft

material holds great promise for the chemical protection coatings, especially under conditions where sustainable healing is required but inaccessible, e.g., in deep sea, arctic regions, and space.

The manufacturing process and features of CuNF heaters are described in Ref. 6. The size of the heater is 50 × 30 mm<sup>2</sup>. In brief, n-hexane was purchased from Sigma-Aldrich and bromobutyl rubber (BIIR) was kindly donated by Lanxess. The BIIR solution was prepared by mixing 22 g of BIIR in 250 ml of n-hexane. Upon the opposite side of heater, a 1.5 ml drop of BIIR solution was dropped and dried in open air for a day on the side of a polyethylene terephthalate (PET) substrate opposite to the CuNF heater side. The thicknesses of the PET substrate and the BIIR layer were 0.09 mm and 0.15 mm, respectively. For the corrosion test, the same CuNF heater was transferred to a steel substrate of 20 × 20 mm<sup>2</sup> in size. The steel substrate was coated with 1 ml of the BIIR solution on the other side (opposite to the side with the CuNF heater) and dried in air for 24 h until the solution was completely solidified.

A pre-notched crack was formed on the BIIR layer on the PET substrate with the CuNF heater underneath using a razor blade (see Fig. 2). Then, the crack was observed with and without (*w/* and *w/o*) the working heater. The heater temperature was controlled by a voltage supplier (Tekpower HY1803D). The optical images were obtained by using an optical microscope (Olympus BX-51), and the surface temperature was measured by using an IR camera (FLIR T1030sc).

The corrosion test was conducted as explained in our previous works.<sup>24,25</sup> The heater fibers were placed on a corrosive steel substrate, and on its other side, a BIIR layer was deposited as an anti-corrosive protecting layer. The BIIR layer was scratched by a razor blade, and the samples were

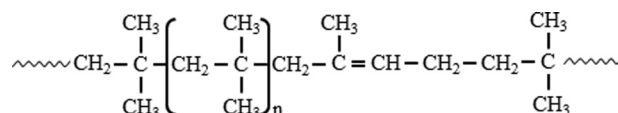


FIG. 1. BIIR chemical structure.

<sup>a)</sup>M. W. Lee and H. S. Jo contributed equally to this work.

<sup>b)</sup>Authors to whom correspondence should be addressed: [yarin@uic.edu](mailto:yarin@uic.edu) and [skyoona@korea.ac.kr](mailto:skyoona@korea.ac.kr)

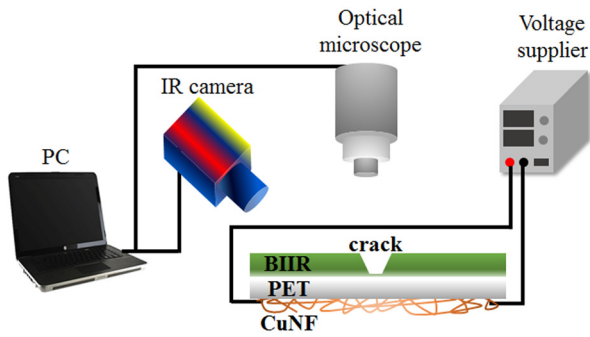


FIG. 2. Schematic of the BIIR-coated CuNF heater and the experimental setup.

dipped in the acetic acid solution for 2 h with and without (*w/* and *w/o*) the heater being on.

To manufacture the CuNF heater, electrospun polyacrylonitrile (PAN) nanofibers (NFs) were used as a template.

Then, they were coated with the Cu layer by electroplating. Before electroplating, the average diameter of PAN NFs was 365 nm, and the size-distribution is shown in Fig. 3(a). Due to deposition of Cu on the surface of PAN NF, the averaged fiber diameter of the fibers was 1.56  $\mu\text{m}$  [Fig. 3(b)], i.e., a fivefold increase was observed.

Figure 3(c) shows the transmittance of the CuNF heater with and without BIIR coating measured by using a UV-VIS spectrophotometer (OPTIZENPOP, Mecasys Co. Ltd., Korea,  $190\text{ nm} \leq \lambda \leq 1100\text{ nm}$ ). Referred to the bare PET substrate (transmittance of 100%), the transmittance of the CuNF heater was 94% at the wavelength of light of  $\lambda = 550\text{ nm}$ . Although the transmittance decreased by about 6% due to the BIIR coating on another side, still a 88% transmittance was measured.

In addition, copper oxidation can accompany heating. Figure 3(d) shows the element map obtained by EDX (energy-dispersive X-ray spectroscopy) (field-emission scan-

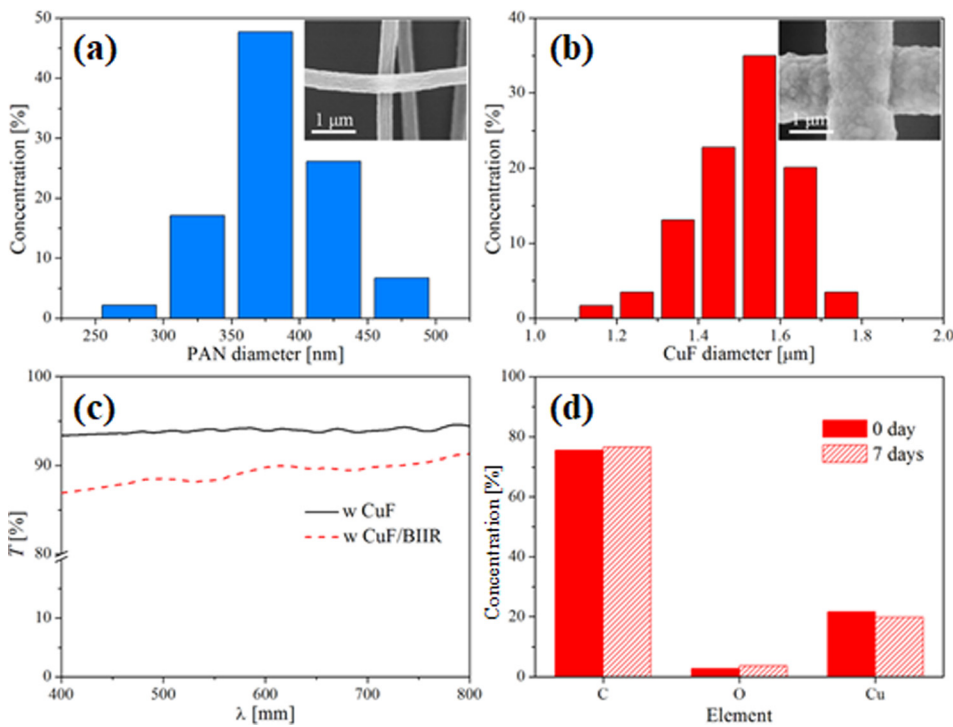


FIG. 3. Diameter distribution of (a) pristine NF and (b) copper-coated fibers. (c) Transparency of the CuNF heater on the PET substrate *w/* and *w/o* BIIR coating. (d) Oxidation of CuNF after 7 days.

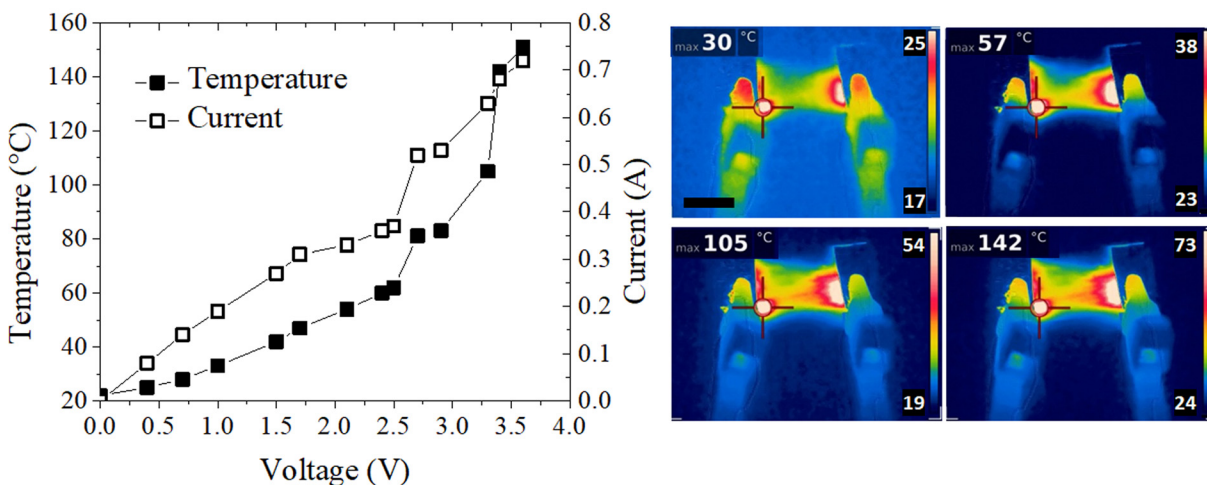


FIG. 4. Temperature and the electric current of the CuNF heater at different applied voltages and the corresponding thermograms, in which the highest temperature value is given in the upper left corner. The scale bar is 1 cm.

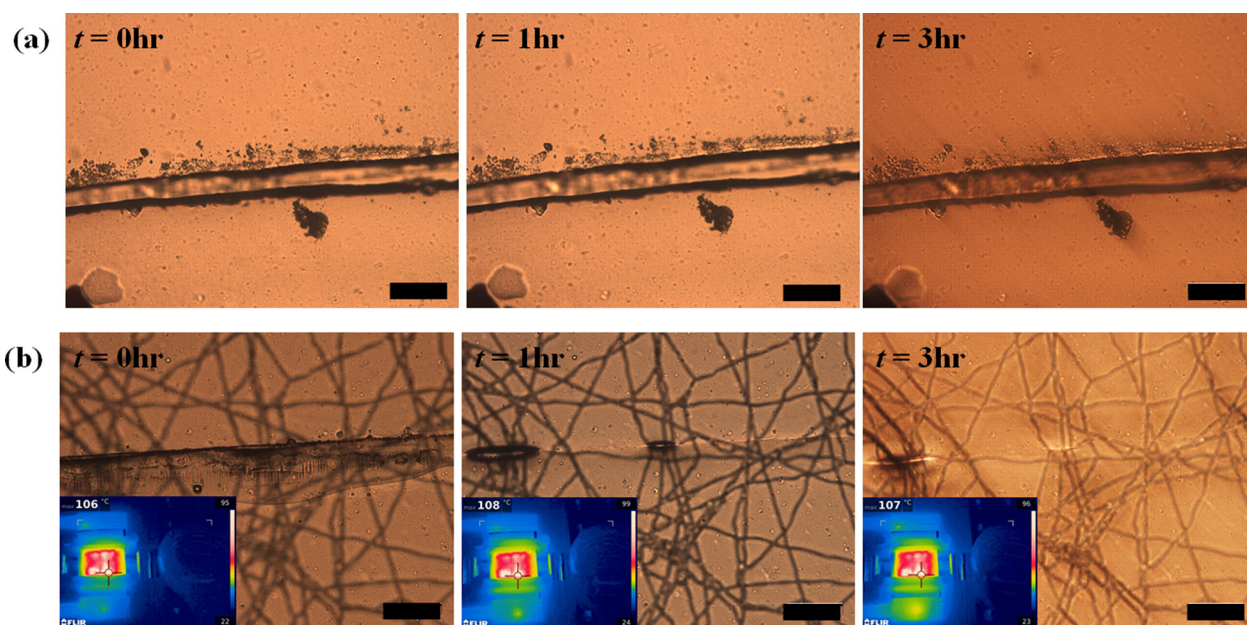


FIG. 5. Optical image of a pre-notched (first) crack on (a) the pristine plane substrate and (b) on the substrate heated with the CuNF heater. Scale bars are 100  $\mu\text{m}$ .

ning electron microscopy, FESEM/EDX, Hitachi S-4800). It reveals that the oxidation of CuNFs was negligible in 7 days, i.e., the concentration of Cu decreased by about 2% and that of O increased by about 1%. This difference was within the error margin, and thus, it was concluded that CuNFs were suitable to be used as a heater.

The heater temperature increased and saturated in 1–2 s after the voltage increase. The temperature values in Fig. 4 correspond to the hottest spot marked by  $\ominus$  in the thermograms. As the voltage increased from 0 to 3.6 V, the surface temperature increased from the room temperature to 151  $^{\circ}\text{C}$ .

A pre-notched crack on the surface of the BIIR layer was observed for the samples w/ and w/o the heater. In particular, the surface temperature of the heater was set at  $\sim 100^{\circ}\text{C}$  at the following current and voltage values on the heater, 1.18 A

and 1.3 V, respectively. Figure 5(a) shows no evolution of the crack without heater. On the other hand, Fig. 5(b) reveals crack healing in 1–3 h at  $T \sim 100^{\circ}\text{C}$  sustained by the heater.

A second pre-notched crack on the BIIR layer surface was created practically on top of the first (healed) one to explore the repeatability of the healing process. Figure 6 shows the cutting marks at  $t = 0\text{h}$  for both samples w/ and w/o heater in panels Figs. 6(a) and 6(b), respectively. The crack in the sample with the operating heater was healed [Fig. 6(b)]. For the sample without the heater, the un-healed crack was visible in 15 days.

The IR thermogram images were recorded before and after a partial cut of a sample (including the heater). Figure 7 shows that heat was not emitted around the cut area of the heater and, accordingly, the damaged BIIR layer could not be healed.

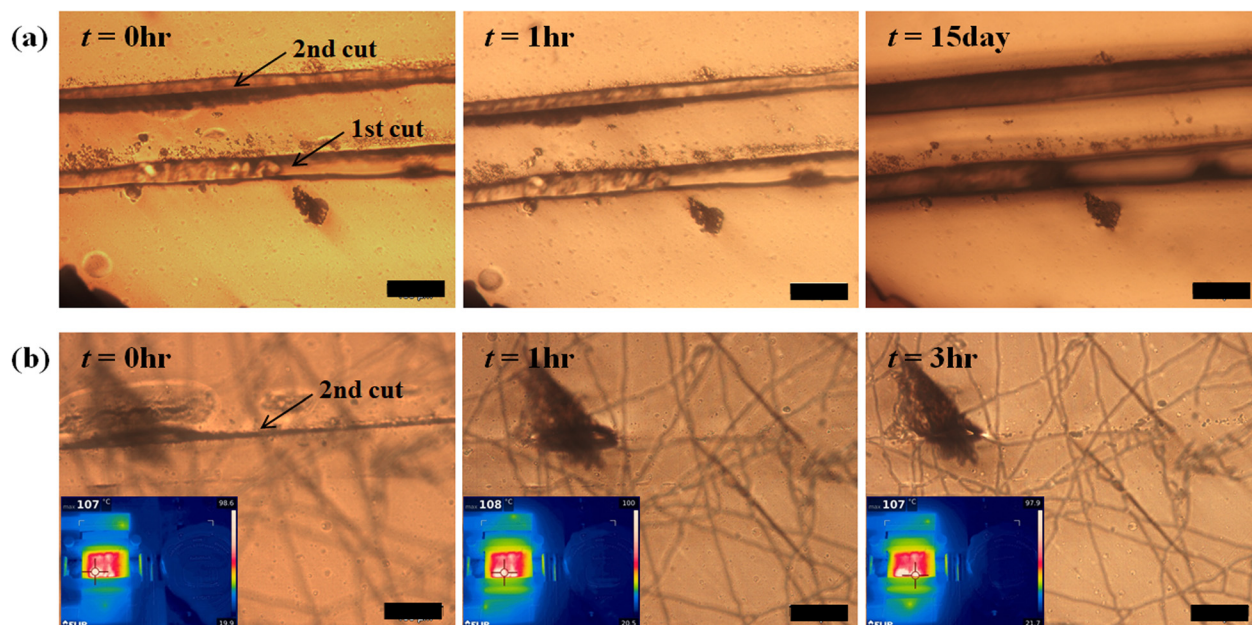


FIG. 6. Optical images of the second crack on (a) the pristine plane substrate and (b) on the substrate heated with the CuNF heater. Scale bars are 100  $\mu\text{m}$ .

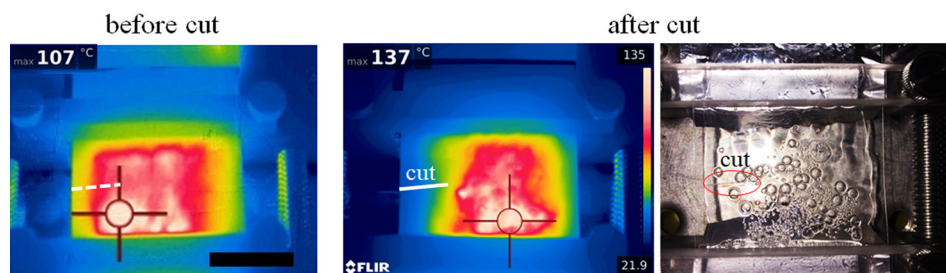


FIG. 7. Thermograms of the partially cut heater and sample. The optical image is on the right. The scale bar is 1 cm.



FIG. 8. Corrosion test in acetic acid: (a) w/ CuNF and (b) w/o CuNF. Time increases from the left-hand-side panels to the right-hand-side panels.

Protective self-healing BIIR coatings can be used on the surface of metal products exposed to a corrosive environment. When a protective layer is damaged, its healing is facilitated by the self-healing coating in a corrosion test, as described below. Two types of steel samples were prepared: one was only covered with a BIIR layer, while the other was covered with a BIIR layer and a heater underneath. The BIIR-covered surfaces of both samples were scratched as “X” as shown in Fig. 8 and left in an open atmosphere for 2 h. Then, 5 ml drops of acetic acid were dripped onto both samples. The sample with a heater powered by the voltage of 2.4 V acquired the surface temperature of about 100 °C. The damaged surfaces of both samples were observed by using a camera for 12 h, as demonstrated in Fig. 8. Although the “X”-shaped scratch is still partially seen on the sample with the heater, the sample was absolutely not corroded since a thin protective layer of BIIR has already been formed [Fig. 8(a)]. On the other hand, the unheated sample gradually oxidized the steel substrate, which was exposed to acetic acid via the un-healed scratch [Fig. 8(b)].

It is demonstrated that Bromobutyl rubber (BIIR) facilitated with transparent electrically conducting Joule heaters comprised of electrospun copper-plated polyacrylonitrile fibers can be used as effective self-healing coatings. They are attractive as a self-healing anti-corrosion protective layer, as well as key elements of transparent stretchable and bendable composite materials and items made of them.

This work was supported by the International Collaboration Program funded by the Agency for Defense Development of the Republic of Korea.

- <sup>1</sup>L. Li, Z. Yu, W. Hu, C.-H. Chang, Q. Chen, and Q. Pei, *Adv. Mater.* **23**(46), 5563 (2011).
- <sup>2</sup>S. Bae, H. Kim, Y. Lee, X. Xu, J.-S. Park, Y. Zheng, J. Balakrishnan, T. Lei, H. R. Kim, Y. I. Song, Y.-J. Kim, K. S. Kim, B. Ozyilmaz, J.-H. Ahn, B. H. Hong, and S. Iijima, *Nat. Nanotechnol.* **5**, 574 (2010).
- <sup>3</sup>D. S. Hecht, L. Hu, and G. Irvin, *Adv. Mater.* **23**(13), 1482 (2011).
- <sup>4</sup>Z. Yu, Q. Zhang, L. Li, Q. Chen, X. Niu, J. Liu, and Q. Pei, *Adv. Mater.* **23**, 664 (2011).
- <sup>5</sup>H. Wu, L. Hu, M. W. Rowell, D. Kong, J. J. Cha, J. R. McDonough, J. Zhu, Y. Yang, M. D. McGehee, and Y. Cui, *Nano Lett.* **10**, 4242 (2010).
- <sup>6</sup>S. An, H. S. Jo, D.-Y. Kim, H. J. Lee, B.-K. Ju, S. S. Al-Deyab, J.-H. Ahn, Y. Qin, M. T. Swihart, A. L. Yarin, and S. S. Yoon, *Adv. Mater.* **28**(33), 7149 (2016).
- <sup>7</sup>H. Wu, D. Kong, Z. Ruan, P.-C. Hsu, S. Wang, Z. Yu, T. J. Carney, L. Hu, S. Fan, and Y. Cui, *Nat. Nanotechnol.* **8**, 421 (2013).
- <sup>8</sup>J.-G. Lee, D.-Y. Kim, J.-H. Lee, S. Sinha-Ray, A. L. Yarin, M. T. Swihart, D. Kim, and S. S. Yoon, *Adv. Funct. Mater.* **27**(1), 1602548 (2017).
- <sup>9</sup>D.-Y. Kim, S. Sinha-Ray, J.-J. Park, J.-G. Lee, Y.-H. Cha, S.-H. Bae, J.-H. Ahn, Y. C. Jung, S. M. Kim, A. L. Yarin, and S. S. Yoon, *Adv. Funct. Mater.* **24**(31), 4986 (2014).
- <sup>10</sup>S. Hong, H. Lee, J. Lee, J. Kwon, S. Han, Y. D. Suh, H. Cho, J. Shin, J. Yeo, and S. H. Ko, *Adv. Mater.* **27**(32), 4744 (2015).
- <sup>11</sup>J.-G. Lee, J.-H. Lee, S. An, D.-Y. Kim, T.-G. Kim, S. S. Al-Deyab, A. L. Yarin, and S. S. Yoon, *J. Mater. Chem. A* **5**(14), 6677 (2017).
- <sup>12</sup>Y. Wang, D. T. Pham, Z. Zhang, J. Li, C. Ji, Y. Liu, and J. Leng, *R. Soc. Open Sci.* **3**, 160488 (2016).
- <sup>13</sup>P. Cordier, F. Tournilhac, C. Soulie-Ziakovic, and L. Leibler, *Nature* **451**, 977 (2008).
- <sup>14</sup>X. Chen, M. A. Dam, K. Ono, A. Mal, H. Shen, S. R. Nutt, K. Sheran, and F. Wudl, *Science* **295**(5560), 1698 (2002).
- <sup>15</sup>N. Bai, G. P. Simon, and K. Saito, *RSC Adv.* **3**, 20699 (2013).
- <sup>16</sup>Y. Li, O. Rios, J. K. Keum, J. Chen, and M. R. Kessler, *ACS Appl. Mater. Interfaces* **8**(24), 15750 (2016).
- <sup>17</sup>Y. Amamoto, H. Otsuka, A. Takahara, and K. Matyjaszewski, *Adv. Mater.* **24**(29), 3975 (2012).
- <sup>18</sup>Y. Amamoto, J. Kamada, H. Otsuka, A. Takahara, and K. Matyjaszewski, *Angew. Chem.* **50**(7), 1660 (2011).
- <sup>19</sup>D.-K. Song, Y.-H. Jo, Y.-J. Lim, S.-Y. Cho, H.-C. Yu, B.-C. Ryu, S.-I. Lee, and C.-M. Chung, *ACS Appl. Mater. Interfaces* **5**(4), 1378 (2013).
- <sup>20</sup>A. Phadke, C. Zhang, B. Arman, C.-C. Hsu, R. A. Mashelkar, A. K. Lele, M. J. Tauber, G. Arya, and S. Varghese, *Proc. Natl. Acad. Sci.* **109**(12), 4383 (2012).
- <sup>21</sup>N. Holtén-Andersen, M. J. Harrington, H. Birkedal, B. P. Lee, P. B. Messersmith, K. Y. C. Lee, and J. H. Waite, *Proc. Natl. Acad. Sci.* **108**(7), 2651 (2011).
- <sup>22</sup>Y. Zhang, A. A. Broekhuis, and F. Picchioni, *Macromolecules* **42**, 1906 (2009).
- <sup>23</sup>A. Das, A. Sallat, F. Bohme, M. Suckow, D. Basu, S. Wießner, K. W. Stockelhuber, B. Voit, and G. Heinrich, *ACS Appl. Mater. Interfaces* **7**, 20623 (2015).
- <sup>24</sup>M. W. Lee, S. An, C. Lee, M. Liou, A. L. Yarin, and S. S. Yoon, *J. Mater. Chem. A* **2**(19), 7045 (2014).
- <sup>25</sup>S. An, M. Liou, K. Y. Song, H. S. Jo, M. W. Lee, S. S. Al-Deyab, A. L. Yarin, and S. S. Yoon, *Nanoscale* **7**, 17778 (2015).